

Functional Expression of M3, a Muscarinic Acetylcholine Receptor Subtype, in Taste Bud Cells of Mouse Fungiform Papillae

Kohgaku Eguchi, Yoshitaka Ohtubo and Kiyonori Yoshii

Department of Brain Science and Engineering, Graduate School of Life Science and Systems Engineering, Kyushu Institute of Technology, Hibikino 2-4, Kitakyushu 808-0196, Japan

Correspondence to be sent to: Kiyonori Yoshii, Hibikino 2-4, Graduate School of Life Science and Systems Engineering, Kyushu Institute of Technology, Kitakyushu 808-0196, Japan. e-mail: yoshii@brain.kyutech.ac.jp

Abstract

Taste bud cells (TBCs) express various neurotransmitter receptors assumed to facilitate or modify taste information processing within taste buds. We investigated the functional expression of muscarinic acetylcholine receptor (mAChR) subtypes, M1–M5, in mouse fungiform TBCs. ACh applied to the basolateral membrane of TBCs elevates the intracellular Ca^{2+} level in a concentration-dependent manner with the 50% effective concentration (EC_{50}) of 0.6 μ M. The Ca^{2+} responses occur in the absence of extracellular Ca^{2+} and are inhibited by atropine, a selective antagonist against mAChRs. The order of 50% inhibitory concentration (IC_{50}) examined with a series of antagonists selective to mAChR subtypes shows the expression of M3 on TBCs. Perforated whole-cell voltage clamp studies show that 1 μ M ACh blocks an outwardly rectifying current and that 100 nM atropine reverses the block. Reverse transcriptase-mediated polymerase chain reaction studies suggest the expression of M3 but not the other mAChR subtypes. Immunohistochemical studies show that phospholipase C β -immunoreactive TBCs and synaptosome-associated protein of 25 kDa-immunoreactive nerve endings are immunoreactive to a transporter that packs ACh molecules into synaptic vesicles (vesicular acetylcholine transporter). These results show that M3 occurs on a few fungiform TBCs and suggest that a few nerve endings, and probably a few TBCs, release ACh by exocytosis. The role of ACh in taste responses is discussed.

Key words: Ca^{2+} imaging, immunohistochemistry, pharmacology, RT-PCR, vesicular acetylcholine transporter, whole-cell clamp

Introduction

Acetylcholine (ACh) is a measure neurotransmitter received by 2 main classes of receptors, the muscarinic ACh receptors (mAChRs) and the nicotinic ones. In the autonomic nervous system, postganglionic parasympathetic neurons release ACh, as postganglionic sympathetic neurons release nor-adrenaline. The involvement of ACh has been suggested in peripheral taste responses, typically in mammals. Physiological studies showed that the intravenous injection of ACh enhanced rat taste nerve responses (Kimura 1961) and that the block of its degradation selectively enhanced the amplitude of the neural responses to sour and salty stimulation in rats (Sakai 1965), though neither the block of ACh degradation nor the application of nicotinic ACh receptor agonists enhanced frog taste nerve responses (Duncan 1964). Also biochemical studies showed that ACh esterase concentration was high in rat taste buds (Paran and Mattern 1975) and that carbachol, an ACh agonist, enhanced inositol turnover in rat lingual tissue (Hwang et al. 1990). Recent studies with Ca^{2+} imaging and immunohistochemical techniques showed the expression of M1, a subtype of 5 mAChR sub-

types M1–M5, on rat and mouse taste bud cells (TBCs) (Ogura 2002; Ogura and Lin 2005). However, the expression of the other mAChR subtypes in TBCs remained to be investigated.

In this study, we investigated the expression of 5 mAChR subtypes in mouse fungiform TBCs and, for comparison, in mouse circumvallate papillae that contained lingual epithelial cells in addition to TBCs with a variety of techniques including reverse transcriptase-mediated polymerase chain reactions (RT-PCR), Ca^{2+} imaging, and perforated whole-cell voltage clamping. Also the expression of a transporter that packs ACh molecules into synaptic vesicles (VAcHT) was investigated, though the expression of VAcHT somewhere in mouse taste tissue was reported in an abstract form without figures (Ogura and Lin 2005). Here, we show that TBCs express M3 and VAcHT and nerve endings express VAcHT in fungiform papillae. Also, we show the expression of VAcHT in circumvallate TBCs and suggest the expression of M1, M3, M4, and M5 in circumvallate papillae. The role of ACh in taste responses is discussed.

Materials and methods

Peeled lingual epithelia

We prepared peeled lingual epithelia containing taste buds in fungiform papillae as described previously (Furue and Yoshii 1997), in accordance with Guiding Principles for the Care and Use of Animals in the Field of Physiological Sciences approved by the Council of the Physiological Society of Japan. In brief, we sacrificed mice by decapitation after anesthetization with ether, removed tongues, and subcutaneously injected them with an elastase solution (the composition of this and other solutions are summarized in Solutions, unless otherwise noted). After 10- to 12-min incubation in Earle's solutions bubbled with 95% O₂/5% CO₂ at 25 °C, we exposed the basolateral membranes of TBCs by peeling the lingual epithelium with forceps, mounted the peeled epithelium on a recording platform with the basolateral membrane side upward, and placed the platform under a 60× water immersion objective (Fluor-60X, Olympus, Tokyo, Japan, Figure 1A). The basolateral membrane side of peeled epithelia was irrigated with either a physiological saline or test solutions by exchanging the composition of the water column between the water immersion objective and the basolateral membrane side. The receptor membrane side facing inside the platform was acclimated to the physiological saline, unless otherwise noted. Peeled lingual epithelia containing circumvallate papillae and those containing no taste buds

(nontaste lingual epithelia) were similarly prepared for RT-PCR and immunohistochemical studies.

Ca²⁺ imaging

After mounting the peeled epithelium on the recording platform, we soaked the basolateral membrane side of the peeled epithelium in a fura-2, acetoxymethyl ester (fura-2 AM) solution for 30 min at 37 °C, washed with the physiological saline, and then placed under a fluorescent microscope equipped with the water immersion objective. ACh and other test substances were dissolved in the physiological solution or in a Ca²⁺-free solution and applied to the basolateral membranes of TBCs (Figure 1A).

Fura-2-stained TBCs were excited at 340 and 380 nm with a spectroscopy-type high-speed wavelength changer (C7773, Hamamatsu Photonics, Hamamatsu, Japan). Images of fura-2 fluorescence were acquired every 2.5 s with an intensified CCD camera through the water immersion objective, stored in a computer, and analyzed with AQUACOSMOS software (version 2.0, Hamamatsu Photonics). Averaged intracellular Ca²⁺ levels, [Ca²⁺]_{in}, over respective cell areas were sequentially plotted as a ratio of F₃₄₀:F₃₈₀. Responses to test solutions were defined as deflections above the mean resting [Ca²⁺]_{in} (obtained by averaging 5 data points during the pretest control period). The response magnitude was calculated as the peak deflection magnitude normalized to the deflection magnitude for 10 μM ACh, and plotted

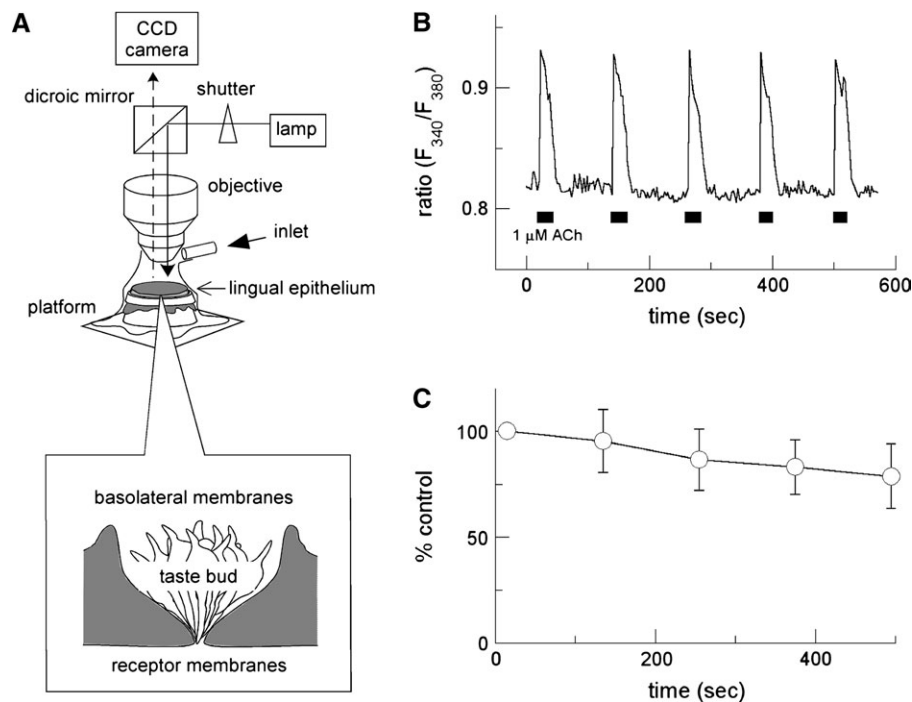


Figure 1 Ca²⁺-imaging scheme (**A**) and Ca²⁺ responses of single fungiform TBCs to 1 μM ACh repetitively applied to the basolateral membrane side of TBCs (**B and C**). Normalized responses, the peak height of each Ca²⁺ response divided by that of the first Ca²⁺ response obtained from their respective TBCs, were plotted as a function of time after the onset of the repetitive stimulation. *n* = 14.

data were mean \pm standard deviation (SD) of these normalized responses, unless otherwise noted.

Isolation of taste buds and purification of taste bud RNA

Lingual epithelia containing fungiform TBCs were peeled as mentioned above except that we injected tongues with an enzyme solution consisting of 0.1% elastase and 0.2% protease dissolved in the physiological saline and that we incubated them in the physiological saline for 4 min at 25 °C. Each peeled epithelium was mounted with the basolateral membrane side upward on the recording platform and was treated with an ethyleneglycol-bis(aminoethylether)-tetraacetic acid (EGTA) solution for 1 min to loosen the connections between taste buds and perigemmal cells, their surrounding tissues. The loosened taste buds were picked up from the peeled epithelia with a micropipette. We collected 30 taste buds for each RT-PCR and extracted total RNA with ISOGEN (Nippon Gene, Tokyo, Japan); we harvested a single taste bud a time and immediately placed it in ISOGEN. Extracted total RNA was incubated with DNase I (Takara Bio, Otsu, Japan) and RNase inhibitor (Takara Bio), in a 20- μ l final volume, to remove any contaminating genomic DNA.

Similarly, we prepared mouse lingual epithelia containing circumvallate papillae, extracted total RNA from the epithelia, and incubated extracted RNA. Note that circumvallate taste buds were not isolated. For positive and negative controls, RNA was extracted from brain tissue and lingual epithelia containing no taste buds.

Reverse transcriptase-mediated polymerase chain reaction

The cDNA synthesis and PCR were carried out using One-Step RT-PCR kit (QIAGEN, Valencia, CA). After isolation of RNA, 1 μ l of total RNA was added to a RT-PCR mix containing 0.6 μ M forward and reverse primers (Table 1). Conditions for RT-PCR were reverse transcription, 55 °C for 30 min; initial PCR activation step, 94 °C for 7.5 min; denaturation, 40 cycles at 94 °C for 30 s; annealing, 54 °C–62 °C for 1 min; extension, 72 °C for 3 min; and final extension, 72 °C for 10 min. Annealing temperatures were 54 °C for M5 and α -gustducin, 58 °C for M1–M4 and β -actin, and 62 °C for VACHT. Optimum annealing temperatures were obtained by preliminary PCR experiments on brain mRNA; we tested a range of annealing temperatures from 50 °C to 62 °C in 4 °C steps and took an annealing temperature that yielded a clear single band with a correct size on agarose gels for each primer set. PCR products were analyzed by 2% agarose gel electrophoresis, stained with ethidium bromide (0.1 μ g/ml), and visualized by UV illumination. PCR products and primers were submitted to Genenet (Fukuoka, Japan), where the identity of the band of interest (PCR product of expected size) was confirmed by sequencing.

Perforated whole-cell voltage clamping

Whole-cell clamp conditions were similar to our previous papers (Ohtubo et al. 2001; Higure et al. 2003) except the

Table 1 Primers used in this study

Gene target	Sequence	Product size (bp)	References
mAChR M1	Forward: 5'-GTAAGGTGCCTGCCATCCAATC-3' Reverse: 5'-CGCAGCTCACTTTCTGCATTGT-3'	417	NM_007698
mAChR M2	Forward: 5'-TGTCAGCAATGCCTCCGTTATG-3' Reverse: 5'-GCCTTGCCATTCTGGATCTTG-3'	480	Zimring et al. 2005
mAChR M3	Forward: 5'-GGTGTGATGATTGGTCTGGCTTG-3' Reverse: 5'-GAAGCAGAGTTTTCCAGGGAG-3'	497	Zimring et al. 2005
mAChR M4	Forward: 5'-TCAAGAGCCCTCTGATGAAGCC-3' Reverse: 5'-AGATTGTCCGAGTCACTTTGCG-3'	477	Zimring et al. 2005
mAChR M5	Forward: 5'-GCTGACCTCCAAGGTCCGATTC-3' Reverse: 5'-CCGTCAGCTTTTACCACCAAT-3'	485	Zimring et al. 2005
VACHT	Forward: 5'-GCCACGTGGATGAAGCACAC-3' Reverse: 5'-GAGGCCACATTACGCAAG-3'	487	NM_021712
α -gustducin	Forward: 5'-CTCTCCAGGAGAAAGTGGC-3' Reverse: 5'-TCAGAAGAGCCCACAGTCTT-3'	248	XM_144196
β -actin	Forward: 5'-GTAAAGACCTCTATGCCAACAC-3' Reverse: 5'-GTGTAACGCAGCTCAGTAAC-3'	289	NM_007393

use of amphotericin B for perforated whole-cell clamping. In brief, electrical responses were recorded with glass electrodes (4–7 M Ω) filled with an amphotericin B electrode solution, amplified with a voltage clamp amplifier (Axopatch 200B, Axon Instruments, Union City, CA), filtered at 10 kHz, digitized with an A/D converter (Digidata 1322A, Axon Instruments), and stored using pCLAMP data acquisition and analysis software (version 8.2, Axon Instruments) on a personal computer. The liquid junction potential of approximately 5 mV between recording and reference electrodes was neglected.

Immunohistochemistry

We immunohistochemically investigated fungiform TBCs in the peeled epithelia without slicing after the fixation and immunohistostaining described as follows. The peel lingual epithelia containing fungiform TBCs were treated with Zamboni solution at 4 °C overnight. After a brief wash in phosphate-buffered saline (PBS), the epithelia were incubated in a citric acid buffer for 20 min at 85 °C. After six 10-min washes with PBS, the epithelia were incubated in a blocking solution containing 3% normal donkey serum, 0.3% Triton X, and 1% bovine serum albumin in PBS for 4 h.

Circumvallate TBCs were transcardially fixed by perfusion with PBS followed by Zamboni solution. The tongue was then postfixed with Zamboni solution for 2 h before incubating with PBS containing 30% sucrose overnight. Circumvallate papilla was embedded in OCT compound (Tissue-Teck, Sakura Finetek Japan, Tokyo, Japan), frozen, and cut with a cryostat into 10- μ m thick sections and immunohistostained.

We incubated the epithelia and sections with primary antibodies (Table 2) dissolved in the blocking solution at 4 °C for 48 h, rinsed with PBS, and incubated with the Alexa Fluor-conjugated secondary antibodies (Table 2) dissolved in the blocking solution at 4 °C overnight. The epithelia were washed with PBS and then mounted on glass slides with 50% glycerol and 0.1 mg/ml *p*-phenylenediamine dissolved in PBS. Fluorescence images of fungiform TBCs in the horizontal, optical slices of whole-mount preparations and those of circumvallate TBCs in 10- μ m thick sections were obtained with a laser scanning confocal microscope system (Leica Microsystems, Bensheim, Germany).

For control purposes, the primary antibody against VAcHT was preadsorbed with a 10-fold molar excess of the synthetic antigen to the normal antibody dilution for 2 h at 37 °C. After the antigen-antibody mixture was spun at 15 000 \times g for 30 min, the supernatant was used for the primary antibody in the usual immunohistochemical protocol.

Solutions

Unless stated otherwise, all reagents for physiological experiments were obtained from Wako (Osaka, Japan). All solu-

Table 2 Antibodies used for immunofluorescence labeling

Antiserum	Type of antibody	Coupled to	Dilution	Origin
Primary				
VAcHT (human)	Goat polyclonal	—	1:500	1
PLC β 2 (human)	Rabbit polyclonal	—	1:100	2
IP $_3$ R3 (human)	Mouse monoclonal	—	1:50	3
SNAP-25 (human)	Mouse monoclonal	—	1:1000	4
Secondary				
Rabbit IgG	Donkey	Alexa Fluor 488	1:400	5
Mouse IgG	Donkey	Alexa Fluor 555	1:400	5
Goat IgG	Donkey	Alexa Fluor 633	1:200	5

1, CHEMICON International, Temecula, CA; 2, Santa Cruz Biotechnology, Santa Cruz, CA; 3, BD Biosciences, San Diego, CA; 4, Sigma-Aldrich, St Louis, MO; 5, Molecular Probes.

tions were prepared with deionized water, and the components were expressed in millimolar concentrations, unless otherwise noted. Physiological saline—150 NaCl, 5 KCl, 2 CaCl $_2$, 0.5 MgCl $_2$, 10 glucose, and 5 HEPES (*N*-2-hydroxyethylpiperazine-*N'*-2-ethanesulfonic acid) (Sigma, St Louis, MO)—buffered to pH 7.4 with NaOH. Amphotericin B electrode solution—130 KCl, 15 NaCl, 5 HEPES, 166 μ g/ml amphotericin B, 250 μ g/ml Pluronic F-127 (Sigma)—buffered to pH 7.2 with KOH. Citric acid buffer—1.8 citric acid monohydrate, 8.2 trisodium citrate dehydrate—buffered to pH 7.0 with NaOH. The Ca $^{2+}$ -free solution was prepared by replacing CaCl $_2$ with MgCl $_2$ in the physiological saline. Earle's solution—116 NaCl, 5.4 KCl, 1.8 CaCl $_2$, 0.8 MgSO $_4$, 26.2 NaHCO $_3$, and 1 NaH $_2$ PO $_4$. EGTA solution—137 NaCl, 2 EGTA, 4 KCl, 10 glucose, and 10 HEPES—buffered to pH 7.4 with NaOH. PBS—137 NaCl, 2.7 KCl, 8.1 Na $_2$ HPO $_4$, and 1.5 KH $_2$ PO $_4$. Phosphate buffer (0.1 M)—80 Na $_2$ HPO $_4$, and 20 NaH $_2$ PO $_4$. Zamboni solution—15% saturated picric acid and 2% paraformaldehyde in the 0.1 M phosphate buffer. The elastase solution was prepared by dissolving 0.1% elastase in the physiological saline. The fura-2 AM solution; 12.5 μ M fura-2 AM (Molecular Probes, Eugene, OR) dissolved in Earle's solution supplemented with 1% Pluronic F-127 (Sigma). Selective mAChR subtype antagonists, 4-diphenylacetoxy-*N*-methylpiperidine methiodide (4-DAMP, M3 antagonist), pirenzepine (M1 antagonist), tropicamide (M4 antagonist), and methoctramine (M2 antagonist) were obtained from Sigma.

Results

Ca $^{2+}$ responses

A subset of TBCs substantially increased [Ca $^{2+}$] $_{in}$ in response to the application of ACh to their basolateral membrane

side, and the repetitive application of 1 μM ACh slightly decreased the Ca^{2+} response in magnitude (Figure 1B,C). The number of TBCs responded to 1 μM ACh per taste bud was 4.9 ± 3.1 cells (mean \pm SD, $n = 32$). Ca^{2+} responses occurred at ACh concentrations lower than 0.01 μM and saturated at concentrations higher than 1 μM , with EC_{50} of 0.6 μM ($n = 38$, Figure 2A,B). In the Ca^{2+} -free solution, Ca^{2+} responses to 1 μM ACh still occurred, though the response magnitude was significantly decreased ($P < 0.01$, repeated measures analysis of variance [ANOVA] and Tukey honestly significant difference (HSD) multiple comparisons test, Figure 2C,D). Also, the resting level of $[\text{Ca}^{2+}]_{\text{in}}$ was decreased in the Ca^{2+} -free solution.

We pharmacologically characterized these Ca^{2+} responses in the presence of a variety of antagonists on the basolateral membrane side (Figure 3). The addition of 100 nM atropine to 1 μM ACh significantly decreased Ca^{2+} responses to $6.7 \pm 4.5\%$ of their respective controls in magnitude ($P < 0.001$, paired Student's *t*-test; $n = 21$), and the wash with the physiological saline partially reversed the inhibition. A series of subtype-selective antagonists inhibited the Ca^{2+} response with different IC_{50} : 1.5 nM for 4-DAMP, an M3 antagonist; 0.1 μM for tropicamide, an M4 antagonist; 1.7 μM for pirenzepine, an M1 antagonist; and 4.0 μM for methoctramine, an M2 antagonist. The order of inhibitory potency agreed with the orders obtained from other tissues expressing M3, mouse duodenal myocytes

(Morel et al. 1997), and guinea pig gallbladder muscles (Parkman et al. 1999) and suggested that M3 was responsible for Ca^{2+} responses.

Perforated whole-cell voltage clamping

We investigated electrical responses of 13 TBCs to 1 μM ACh selectively applied to their basolateral membranes under a perforated whole-cell clamp condition (Figure 4). The application partially inhibited the magnitude of a voltage-gated outwardly rectifying current in one TBC, though that current remained unchanged in the other TBCs. The ACh-sensitive current developed very slowly at membrane potentials more positive than -20 mV, lasted for more than 50 ms without inactivation, and was antagonized by the addition of 100 nM atropine to the ACh solution.

PCR studies

We also investigated the expression of mAChR subtypes on fungiform TBCs with RT-PCR and detected a PCR product for M3 (Figure 5). The product size agreed with the expected one, and the identity of the product was confirmed by sequencing. RT-PCR products for the other mAChR subtypes, M1, M2, M4, M5, and VAChT, were undetectable. These results were consistent with the pharmacological results mentioned above.

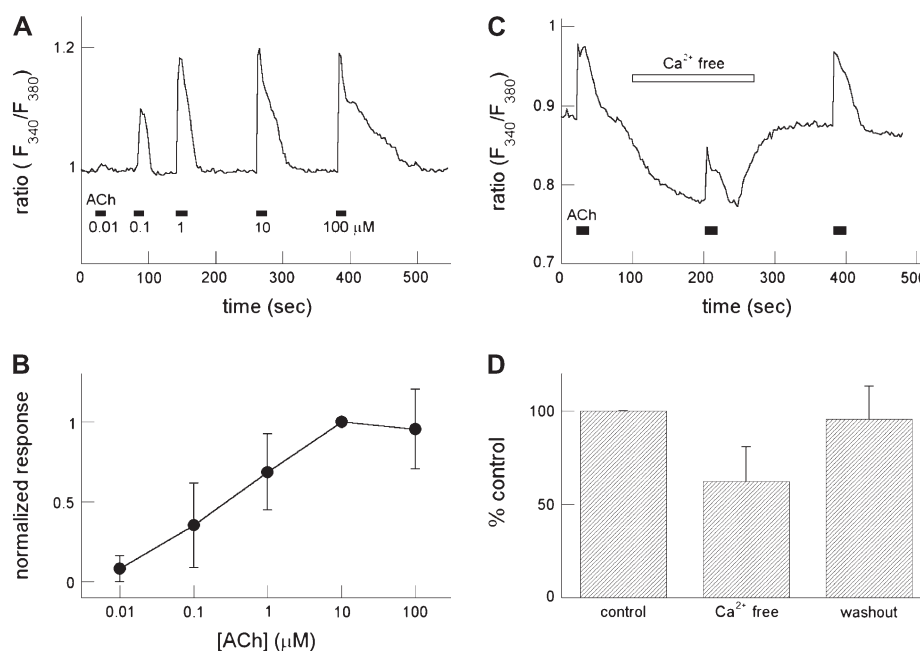


Figure 2 Ca^{2+} responses recorded under different conditions. **(A)** Ca^{2+} responses of a fungiform TBC to a concentration series of ACh. **(B)** Concentration-response relationship for ACh. Ca^{2+} responses were calculated relative to the magnitude of the response to 10 μM ACh in each TBC. EC_{50} , 0.55 ± 0.71 μM ($n = 38$). **(C)** Typical Ca^{2+} responses to 1 μM ACh in a Ca^{2+} -free solution. The basolateral membrane side was acclimated to the Ca^{2+} -free solution, irrigated with 10 μM ACh dissolved in the Ca^{2+} -free solution, and washed with the Ca^{2+} -free solution. **(D)** Ca^{2+} responses to 10 μM ACh in the Ca^{2+} -free solution. The magnitude of Ca^{2+} responses examined in the Ca^{2+} -free solution and that in the physiological saline after the wash was calculated relative to the magnitude of Ca^{2+} responses recorded in the physiological saline before the irrigation with the Ca^{2+} -free solution. The magnitude of Ca^{2+} responses was significantly smaller in the Ca^{2+} -free solution than in the physiological saline ($*P < 0.01$, repeated measures ANOVA and Tukey HSD multiple comparisons test, $n = 16$).

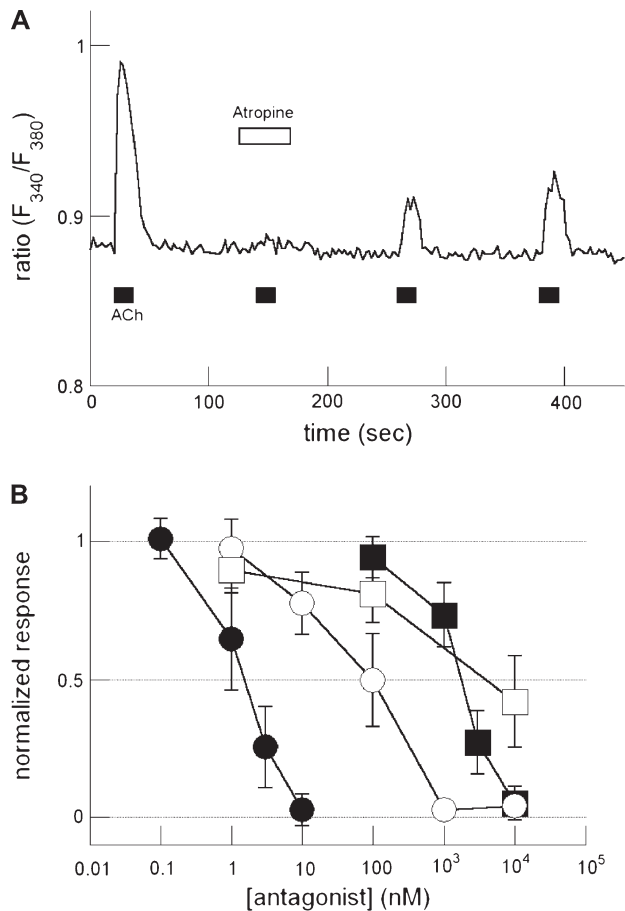


Figure 3 Inhibition of Ca^{2+} responses by muscarinic antagonists. **(A)** Typical responses of a single TBC to $1 \mu\text{M}$ ACh in the presence of $0.1 \mu\text{M}$ atropine. **(B)** Inhibition curves of subtype-specific antagonists for Ca^{2+} responses to $1 \mu\text{M}$ ACh. Closed circles, 4-DAMP; open circles, tropicamide; closed squares, pirenzepine; and open squares, methoctramine. The magnitude of Ca^{2+} responses was calculated as relative to that in the absence of antagonists in each TBC. Each point of data is obtained from 3 to 15 TBCs.

For comparison, we investigated the expression of mAChR subtypes and VACHT in circumvallate papillae that contained taste buds and surrounding lingual epithelial cells. PCR products detected were for M1, M3, M4, M5, and VACHT, but those for M2 were undetectable (data not shown).

Immunohistostaining

In fungiform papillae, there were immunoreactive regions to an anti-VACHT antibody in horizontal, optical slices of whole-mount taste buds (Figure 6). No immunoreactivity was detected after preadsorption of the anti-VACHT antibody with the synthetic antigen. Shifting the focal plane of confocal microscopy, we found that VACHT immunoreactivity occurred on a few PLC β 2-immunoreactive TBCs and that a few nerve endings, SNAP-25-immunoreactive regions having no soma-like bulges within taste buds, were also immunoreactive to both VACHT and SNAP-25. Also,

we investigated VACHT immunoreactivity in circumvallate taste buds with sliced preparations (see Materials and methods). VACHT immunoreactivity occurred on a few inositol 1,4,5-triphosphate receptor, type III (IP $_3$ R3)-immunoreactive TBCs, but that on SNAP-25-immunoreactive TBCs was undetectable.

Discussion

The present results obtained with Ca^{2+} imaging, RT-PCR, and perforated whole-cell clamping cooperatively showed that fungiform TBCs expressed M3 as follows. The order of inhibitory potency yielded by Ca^{2+} imaging was 4-DAMP > tropicamide > pirenzepine > methoctramine (Figure 3B), which agreed with the order obtained from other tissues expressing M3, mouse duodenal myocytes (Morel et al. 1997), and guinea pig gallbladder muscles (Parkman et al. 1999). Only one RT-PCR product detected in fungiform TBCs was for M3 (Figure 5). A current obtained from a fungiform TBC assumed to be M-current as described later supports the expression of M3 (Figure 4) because M-current can be modulated by M3 (Marrion 1997).

The present study also suggests that TBCs or epithelial cells in circumvallate papillae express M1, M3, M4, and M5. These results agreed with previous results that immunohistochemically showed the expression of M1 in foliate and circumvallate TBCs, though the expression of mAChR subtypes other than M1 had not been examined (Ogura 2002; Ogura and Lin 2005). It is thus likely that fungiform and circumvallate TBCs express different mAChR subtypes. The responsiveness of the chorda tympani nerve innervating fungiform TBCs is different from that of the glossopharyngeal nerve innervating circumvallate TBCs (Sako et al. 2000). The subtype of mAChRs on TBCs may contribute to the differences.

M3 as well as M1 and M5 coupled to the α subunit of $G_{q/11}$ class G proteins results in the increase in $[\text{Ca}^{2+}]_{\text{in}}$ via the activation of PLC β 2, whereas M2 and M4 are coupled to $G_{i/o}$ class G proteins and decrease intracellular cyclic adenosine 3',5'-monophosphate levels (Caulfield 1993; Caulfield et al. 1994; Felder 1995). Type II cells, partially identical to PLC β 2-immunoreactive TBCs, express G protein-coupled taste receptors, T1Rs and T2Rs, which are coupled to the activation of PLC β 2 (Zhang et al. 2003). Because the α subunit of $G_{q/11}$, $G_{\alpha q}$, was expressed in rat TBCs (Kusakabe et al. 2000), it is likely that the present ACh-induced Ca^{2+} responses occur in Type II cells that express M3. This cross talk between G protein-coupled taste receptors and M3 would enhance the taste response of these Type II cells, when ACh is applied to them during taste stimulation. This hypothesis may account for previous results (Kimura 1961; Sakai 1965).

The present study detected VACHT immunoreactivity in fungiform and circumvallate taste buds (Figure 6), suggesting that TBCs or nerve endings release ACh by exocytosis. VACHT-immunoreactive TBCs were PLC β 2 immunoreactive

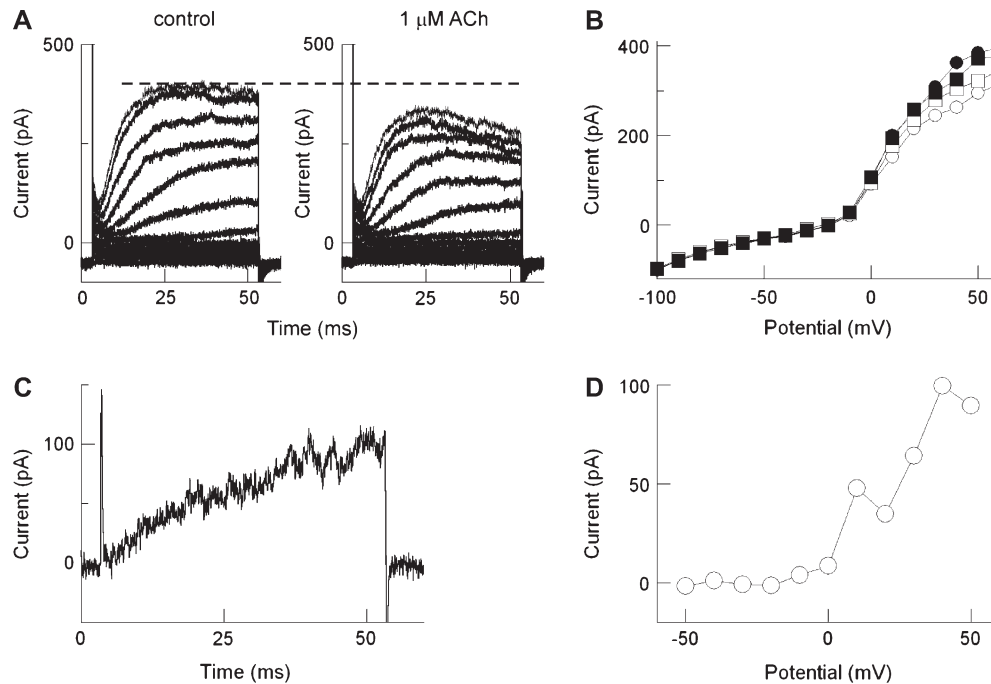


Figure 4 Voltage-gated outwardly rectifying currents of a fungiform TBC inhibited by ACh. **(A)** A family of voltage clamp currents. The voltage steps range from -50 to 50 mV in 10 -mV increments from a holding potential of -70 mV. **(B)** Current-voltage relations recorded before (closed circles), during the application of $1 \mu\text{M}$ ACh (open circles), during the application of $1 \mu\text{M}$ ACh in the presence of 100 nM atropine (open squares), and after wash with the physiological saline (closed squares). **(C)** ACh-sensitive currents elicited by a test potential to 50 mV from a holding potential of -70 mV. The ACh-sensitive currents are obtained by subtracting record without $1 \mu\text{M}$ ACh from record with it. **(D)** Current-voltage relation for ACh-sensitive currents obtained by the subtraction as in **(C)**.

in fungiform taste buds and were $\text{IP}_3\text{R}3$ immunoreactive in circumvallate taste buds. Although RT-PCR failed to detect VAcHT in fungiform taste buds, the failure seems to result from the fact that the number of fungiform taste buds used in the RT-PCR study was much smaller than that of circumvallate taste buds.

Both $\text{PLC}\beta 2$ -immunoreactive TBCs and $\text{IP}_3\text{R}3$ -immunoreactive TBCs are assumed to be Type II cells, which have no synaptic vesicles. Also, these VAcHT-immunoreactive Type II-like cells expressed no SNAP-25. It appears that these TBCs cannot release ACh by exocytosis. However, immunohistochemical classification is different from morphological classification, and not all $\text{PLC}\beta 2$ -immunoreactive TBCs and $\text{IP}_3\text{R}3$ -immunoreactive TBCs are classified into Type II (Clapp et al. 2004). Also, VAcHT-immunoreactive Type II-like cells may express another member of SNAP family. Therefore, further studies are needed to elucidate the role of VAcHT in these TBCs.

VAcHT immunoreactivity was also detected in SNAP-25-immunoreactive nerve endings in fungiform taste buds, suggesting that these nerve endings release ACh by exocytosis using SNAP-25, which generates muscarinic actions on TBCs via M3. VAcHT-immunoreactive nerve endings may be postganglionic parasympathetic nerves because they innervated TBCs in bullfrogs (Sato et al. 2005). Similar muscarinic

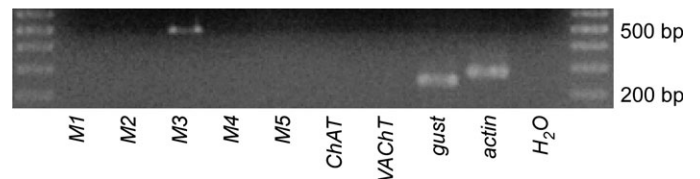


Figure 5 PCR-amplified products from cDNA reverse transcribed from mRNA isolated from fungiform TBCs. Oligonucleotide primers specific for 5 different mAChR subtypes are run in separate reactions, and the products are run on agarose gel electrophoresis. The sequences of primers and expected product size of each reaction are listed in Table 1. Oligonucleotide primers specific for β -actin and α -gustducin are similarly examined as positive controls. H_2O used in RT-PCR experiments is also examined as a negative control. Identical aliquots of a single mRNA for each tissue were used as templates for the RT-PCR reactions shown. Identical results were obtained with 3 additional preparations of RNA from taste buds.

actions may occur on circumvallate TBCs. Rat circumvallate and foliate TBCs expressed adrenergic receptors where noradrenaline inhibited voltage-gated outward potassium currents (Herness et al. 2002). It is thus likely that both sympathetic and parasympathetic neurons supply TBCs and modulate their functions as found in a variety of organs.

The current obtained from a fungiform TBC was sensitive to ACh and atropine, slowly activated at membrane

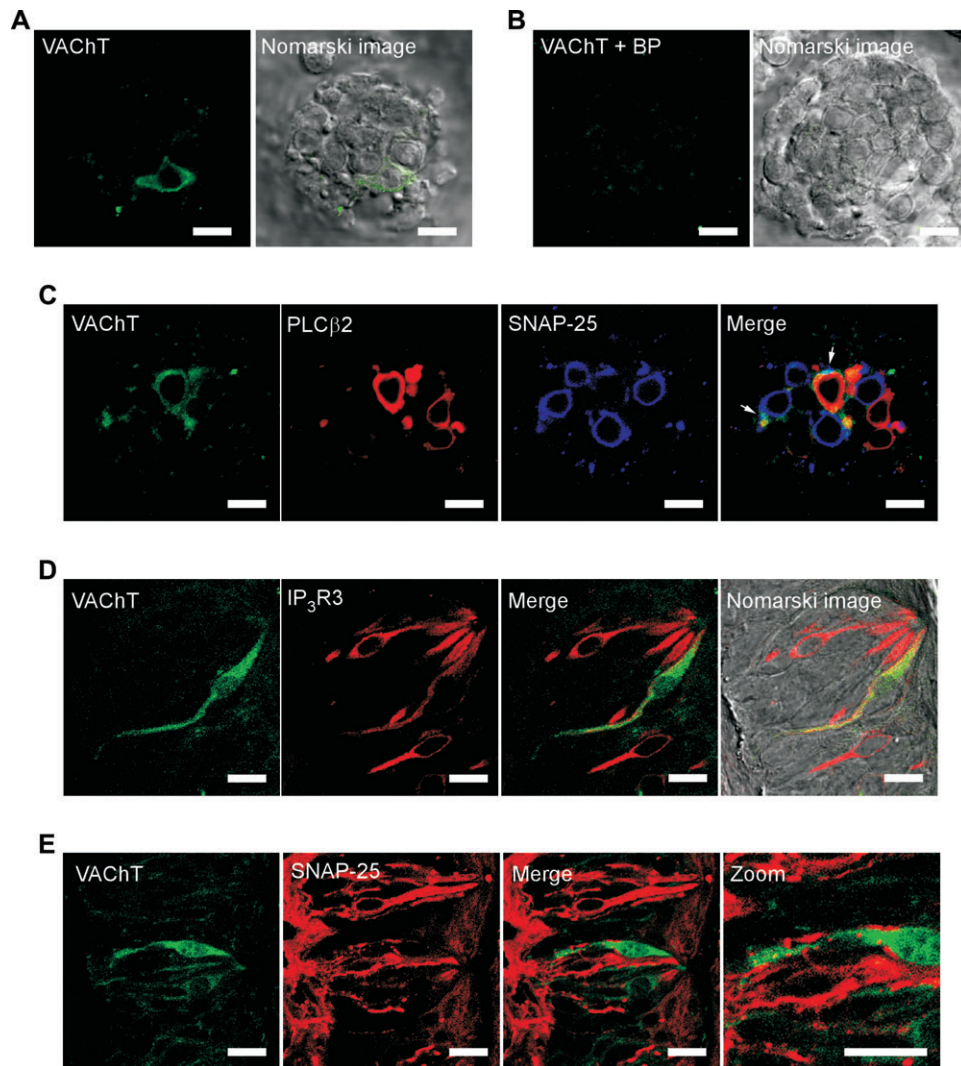


Figure 6 Immunohistochemical images of VACHT in fungiform taste buds (**A–C**) and in circumvallate taste buds (**D**). (**A**) Immunofluorescence of VACHT (green) and their overlay on a Nomarski image of the same section. (**B**) No selective labeling was observed in control section, in which the primary antibody was preadsorbed with the synthetic antigen. (**C**) Immunofluorescence of VACHT (green), PLC β 2 (red), SNAP-25 (blue), and their overlay on a Nomarski image of the same section. Immunoreactivity for VACHT occurs on PLC β 2-immunoreactive TBCs and SNAP-25-immunoreactive nerve endings (arrows). (**D**) Immunofluorescence of VACHT (green), IP $_3$ R3 (red) and their overlay, and the overlay on a Nomarski image of the same section. VACHT immunoreactivity occurs on IP $_3$ R3-immunoreactive TBCs. (**E**) Immunofluorescence of VACHT (green), SNAP-25 (red), their overlay, and the enlargement of the overlay. No VACHT immunoreactivity occurs on SNAP-25-immunoreactive TBCs. Scale bar = 10 μ m.

potentials less than -20 mV, and noninactivated. These properties except the range of activation potentials are similar to M-current previously reported (Adams et al. 1982), showing that the current is M-current. Suppression of M-current usually results in membrane depolarization and an increase in input resistance, which makes the cell more likely to fire action potentials. In TBCs, its suppression would not depolarize the TBC at resting potentials because of its higher activation potentials. Although the TBC that generated M-current exhibited no voltage-gated Na $^+$ currents, M-current may occur on Type II cells that fire action potential. When this is the case, the suppression of M-current elongated the action potential of the TBC.

In response to taste substances, TBCs generate action potentials that open hemichannels and ATP as a neurotransmitter is released through the hemichannels (Finger et al. 2005; Huang et al. 2007; Romanov et al. 2007). Therefore, the suppression of M-current facilitates the ATP release, which results in the enhancement of taste nerve responses, which agree with previous studies (Kimura 1961; Sakai 1965). The channels that elicit the M-current of TBCs remain to be identified. Two voltage-gated channels, KCNQ1 and KCNH2, were found in rat TBCs in circumvallate papillae (Ohmoto et al. 2006). These channels may be responsible for the M-current of TBCs because KCNQ1 and probably KCNH2 generate M-current (Jentsch 2000).

Funding

21st Centre of Excellence Program (center J19), Kyushu Institute of Technology; Japan Society for the Promotion of Science (Grants-in-Aid for Scientific Research #16300094).

References

- Adams PR, Brown DA, Constanti A. 1982. M-currents and other potassium currents in bullfrog sympathetic neurones. *J Physiol.* 330:537–572.
- Caulfield MP. 1993. Muscarinic receptors—characterization, coupling and function. *Pharmacol Ther.* 58:319–379.
- Caulfield MP, Jones S, Vallis Y, Buckley NJ, Kim GD, Milligan G, Brown DA. 1994. Muscarinic M-current inhibition via G alpha q/11 and alpha-adrenoceptor inhibition of Ca²⁺ current via G alpha o in rat sympathetic neurones. *J Physiol.* 477(Pt 3):415–422.
- Clapp TR, Yang R, Stoick CL, Kinnamon SC, Kinnamon JC. 2004. Morphologic characterization of rat taste receptor cells that express components of the phospholipase C signaling pathway. *J Comp Neurol.* 468:311–321.
- Duncan CJ. 1964. Synaptic transmission at taste buds. *Nature.* 203:875–876.
- Felder CC. 1995. Muscarinic acetylcholine receptors: signal transduction through multiple effectors. *FASEB J.* 9:619–625.
- Finger TE, Danilova V, Barrows J, Bartel DL, Vigers AJ, Stone L, Hellekant G, Kinnamon SC. 2005. ATP signaling is crucial for communication from taste buds to gustatory nerves. *Science.* 310:1495–1499.
- Furue H, Yoshii K. 1997. In situ tight-seal recordings of taste substance-elicited action currents and voltage-gated Ba currents from single taste bud cells in the peeled epithelium of mouse tongue. *Brain Res.* 776:133–139.
- Herness S, Zhao FL, Kaya N, Lu SG, Shen T, Sun XD. 2002. Adrenergic signaling between rat taste receptor cells. *J Physiol.* 543:601–614.
- Higure Y, Katayama Y, Takeuchi K, Ohtubo Y, Yoshii K. 2003. Lucifer Yellow slows voltage-gated Na⁺ current inactivation in a light-dependent manner in mice. *J Physiol.* 550:159–167.
- Huang YJ, Maruyama Y, Dvoryanchikov G, Pereira E, Chaudhari N, Roper SD. 2007. The role of pannexin 1 hemichannels in ATP release and cell-cell communication in mouse taste buds. *Proc Natl Acad Sci USA.* 104:6436–6441.
- Hwang PM, Verma A, Brecht DS, Snyder SH. 1990. Localization of phosphatidylinositol signaling components in rat taste cells: role in bitter taste transduction. *Proc Natl Acad Sci USA.* 87:7395–7399.
- Jentsch TJ. 2000. Neuronal KCNQ potassium channels: physiology and role in disease. *Nat Rev Neurosci.* 1:21–30.
- Kimura K. 1961. Factors affecting the response of taste receptors of rat. *Kumamoto Med J.* 14:95–99.
- Kusakabe Y, Yasuoka A, Asano-Miyoshi M, Iwabuchi K, Matsumoto I, Arai S, Emori Y, Abe K. 2000. Comprehensive study on G protein alpha-subunits in taste bud cells, with special reference to the occurrence of Galphai2 as a major Galpha species. *Chem Senses.* 25:525–531.
- Marrion NV. 1997. Control of M-current. *Annu Rev Physiol.* 59:483–504.
- Morel JL, Macrez N, Mironneau J. 1997. Specific Gq protein involvement in muscarinic M3 receptor-induced phosphatidylinositol hydrolysis and Ca²⁺ release in mouse duodenal myocytes. *Br J Pharmacol.* 121:451–458.
- Ogura T. 2002. Acetylcholine increases intracellular Ca²⁺ in taste cells via activation of muscarinic receptors. *J Neurophysiol.* 87:2643–2649.
- Ogura T, Lin W. 2005. Acetylcholine and acetylcholine receptors in taste receptor cells. *Chem Senses.* 30(Suppl 1):i41.
- Ohmoto M, Matsumoto I, Misaka T, Abe K. 2006. Taste receptor cells express voltage-dependent potassium channels in a cell age-specific manner. *Chem Senses.* 31:739–746.
- Ohtubo Y, Suemitsu T, Shiobara S, Matsumoto T, Kumazawa T, Yoshii KY. 2001. Optical recordings of taste responses from fungiform papillae of mouse in situ. *J Physiol.* 530:287–293.
- Paran N, Mattern CF. 1975. The distribution of acetylcholinesterase in buds of the rat vallate papilla as determined by electron microscope histochemistry. *J Comp Neurol.* 159:29–44.
- Parkman HP, Pagano AP, Ryan JP. 1999. Subtypes of muscarinic receptors regulating gallbladder cholinergic contractions. *Am J Physiol.* 276:G1243–G1250.
- Romanov RA, Rogachevskaja OA, Bystrova MF, Jiang P, Margolskee RF, Kolesnikov SS. 2007. Afferent neurotransmission mediated by hemichannels in mammalian taste cells. *EMBO J.* 26:657–667.
- Sakai K. 1965. Studies on chemical transmission in taste fibre endings. II. The effect of Cholinesterase inhibitor on the taste. *Chem Pharm Bull (Tokyo).* 13:304–307.
- Sako N, Harada S, Yamamoto T. 2000. Gustatory information of umami substances in three major taste nerves. *Physiol Behav.* 71:193–198.
- Sato T, Okada Y, Miyazaki T, Kato Y, Toda K. 2005. Taste cell responses in the frog are modulated by parasympathetic efferent nerve fibers. *Chem Senses.* 30:761–769.
- Zhang Y, Hoon MA, Chandrashekar J, Mueller KL, Cook B, Wu D, Zuker CS, Ryba NJ. 2003. Coding of sweet, bitter, and umami tastes: different receptor cells sharing similar signaling pathways. *Cell.* 112:293–301.
- Zimring JC, Kapp LM, Yamada M, Wess J, Kapp JA. 2005. Regulation of CD8+ cytolytic T lymphocyte differentiation by a cholinergic pathway. *J Neuroimmunol.* 164:66–75.

Accepted August 8, 2007